AIAA JOURNAL
Vol. 30, No. 11, November 1992

Technical Notes

TECHNICAL NOTES are short manuscripts describing new developments or important results of a preliminary nature. These Notes cannot exceed 6 manuscript pages and 3 figures; a page of text may be substituted for a figure and vice versa. After informal review by the editors, they may be published within a few months of the date of receipt. Style requirements are the same as for regular contributions (see inside back cover).

Implementation of Vigneron's Streamwise Pressure Gradient Approximation in Parabolized Navier-Stokes Equations

Joseph H. Morrison*
Analytical Services and Materials, Inc., Hampton, Virginia 23666
and
John J. Korte†
NASA Langley Research Center, Hampton, Virginia 23681

Introduction

THE work of Vigneron et al.[1] determined the fraction ω of the subsonic streamwise pressure gradient that could be retained in the parabolized Navier-Stokes (PNS) equations to maintain a stable marching procedure for viscous supersonic flowfields. Vigneron's approximation has become the preferred method for modifying the subsonic streamwise pressure gradient when space marching the PNS equations. An investigation into the implementation of this approximation in PNS schemes has uncovered two sources of error. The two errors can cause significant errors in the temperature profile and skin-friction coefficient. These two errors and a strategy for correcting them will be explained and demonstrated for a supersonic flat-plate flowfield.

Vigneron's Approximation

The Navier-Stokes equations are not parabolic because of the upstream influence allowed through the streamwise pressure gradient term. Vigneron et al.[1] parabolized these equations by splitting the streamwise pressure gradient into two parts:

$$\frac{\partial p}{\partial x} = \omega \frac{\partial p}{\partial x} + (1-\omega)\frac{\partial p}{\partial x} \tag{1}$$

where p is the pressure and x the streamwise coordinate. The portion $\omega \partial p/\partial x$ is solved with the flow variables, and the rest of the pressure gradient is treated as a source term or dropped.

The coefficient ω is determined from an eigenvalue analysis of the equations and represents the fraction of the streamwise pressure gradient that can be retained in the subsonic region to achieve a parabolic equation. The result of the eigenvalue analysis is that the inviscid eigenvalues are real and the viscous eigenvalues are real and positive if

$$u > 0 \tag{2}$$

and

$$\omega = \begin{cases} 1 & M_x \geq 1 \\ \dfrac{\gamma M_x^2}{1+(\gamma-1)M_x^2} & M_x < 1 \end{cases} \tag{3}$$

where $M_x = u/a$ is the Mach number in the x direction, a the speed of sound, and γ the ratio of specific heats. In practice, ω is implemented with a safety factor σ multiplying Eq. (3) to allow for nonlinearities not accounted for in the eigenvalue analysis. Typical values for σ are between 0.75 and 0.95.

Numerical Implementation

The streamwise flux gradient is evaluated in an implicit finite difference or finite volume scheme using a first-order backward difference. Implicit algorithms lag the value of ω at the previous cross section as the first-order spatial integration is performed. This results in ω being constant along grid lines in the streamwise direction. Recent advances have created algorithms that use higher-order spatial differencing and no longer lag the value of ω, thereby using a different value of ω for each grid point. A difficulty arises in these new schemes: the use of the conservative form of the equation, coupled with the nonconstant value of ω, leads to the streamwise pressure term being differenced as

$$\frac{\partial(\omega p)}{\partial x} \tag{4}$$

The chain rule for differentiation shows that

$$\frac{\partial(\omega p)}{\partial x} = \omega \frac{\partial p}{\partial x} + p \frac{\partial \omega}{\partial x} \tag{5}$$

The result is that the parabolized equations solved in this form do not have the same behavior as the Navier-Stokes equations that they were derived from. This can easily be seen for supersonic flow past a flat plate aligned with the flowfield. For the flat-plate flow the streamwise pressure gradient is $\partial p/\partial x \approx 0$ (away from the leading edge). Recall that the classical boundary-layer assumption is $\partial p/\partial y \approx 0$ (where y is normal to the plate). Therefore, the pressure is nearly constant on the plate, and the pressure derivative terms do not contribute to the equations. However, $\partial(\omega p)/\partial x$ is not zero when ω is not constant. Rather, this term depends on the grid used due to the dependence of ω on M_x^2. Thus, not only is there a nonphysical acceleration of the flow due to the ω term, but it is grid dependent.

There are two potential solutions to this problem: 1) implement the scheme whereby ω is constant for the two fluxes evaluated; or 2) subtract the $p\,\partial\omega/\partial x$ term. A second difficulty arises in PNS schemes in generalized coordinates, such as the scheme developed by Newsome et al.,[2] which use a finite volume stencil. This is best illustrated again for the flat-plate case. As stated earlier, the pressure is approximately constant

Presented as Paper 92-0189 at the AIAA 30th Aerospace Sciences Meeting, Reno, NV, Jan. 6-9, 1992; received Feb. 11, 1992; revision received May 6, 1992; accepted for publication May 7, 1992.

*Research Scientist, 107 Research Dr. Member AIAA.
†Senior Research Scientist, Theoretical Flow Physics Branch, Fluid Mechanics Division, Mail Stop 156. Senior Member AIAA.

over the flat plate. Figure 1 shows a control volume with the pressure terms acting on each face. In the subsonic region of the boundary layer, the left and right faces of the control volume are acted on by a portion of the pressure due to Vigneron's approximation, whereas the top and bottom of the control volume are acted on by the entire pressure term. A surface integral of the pressure should be zero, but because of differing areas acted on by the pressure p on the top and bottom and the ωp terms on the left and right faces, another nonphysical acceleration results. This second difficulty can be corrected by including the geometric conservation law that several researchers have implemented.[3]

Korte[4] has developed a finite difference scheme that overcomes the two aforementioned difficulties by implementing the geometric conservation law and subtracting the $p\partial\omega/\partial x$ term. Morrison and Korte[5] describe a finite volume procedure that overcomes the errors by rewriting the PNS equations with the full streamwise flux and an additional source term $\omega\partial P/\partial x$ included. The net effect of using the sum is to account for Vigneron's approximation. The source term is evaluated with a cell constant value of ω and uses the divergence theorem to evaluate $\partial p/\partial x$.

Results

The test case is supersonic laminar flow over a flat plate. The flow conditions are chosen to match those of Lawrence et al.[6]: freestream Mach number $= 2.0$, Reynolds number $= 1.65 \times 10^6$, Prandtl number $= 0.72$, freestream temperature and wall temperature $= 222$ K, safety factor $\sigma = 0.95$, and plate length $L = 1$ m. The computations were done on two grids with 51 and 101 points normal to the plate. The iterative scheme used 51 and 101 uniformly spaced cross sections, respectively, and the explicit scheme marched with a Courant-Friedrichs-Lewy (CFL) number of 1.

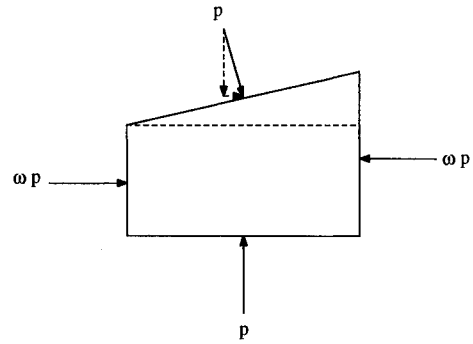

Fig. 1 Control volume for pressure balance.

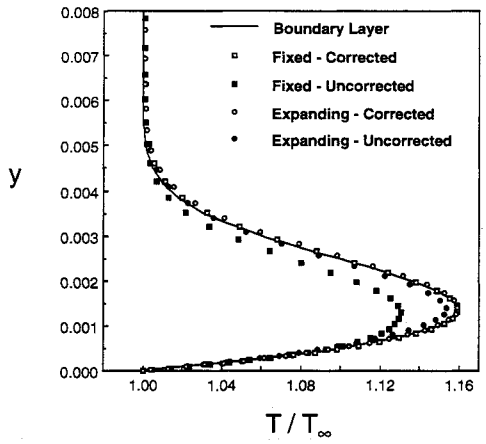

Fig. 2 Comparison of temperature profiles at $x = 0.93$ m.

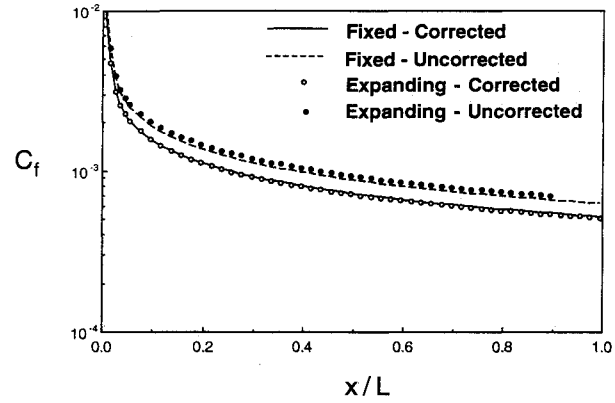

Fig. 3 Comparison of skin-friction coefficient.

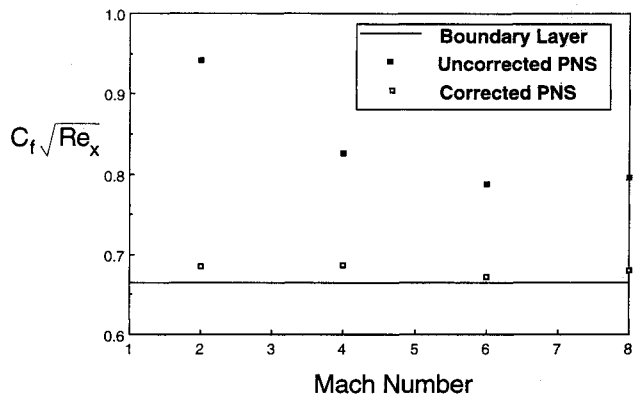

Fig. 4 Comparison of skin-friction coefficient for a linear viscosity law, adiabatic wall.

Grid Effects

Two different grids were run: 1) the outer boundary fixed at $y_{max} = 0.8$ and 2) the outer boundary growing linearly from $y_{max} = 0.06$ at $x = 0$ to $y_{max} = 0.8$ at $x = L$. The results shown are for the iterative, finite volume scheme only. The results for the finite difference scheme are almost identical and are not shown for conciseness. Figures 2 and 3 show the results of the computations on the test case without and with the correction. Results are compared to the solution from a boundary-layer computation.[7] Results for the fine mesh only are presented here for conciseness. The coarse grid calculations give essentially the same results, demonstrating that the calculations are grid converged and that the difference is not due to a grid convergence issue. Figure 2 shows the temperature profile on the two meshes at $x = 0.93L$. The uncorrected form of the equations differs from the boundary-layer solution in the following ways: The velocity profile is too full[5] and the peak value of the temperature is underpredicted. The corrected form fixes these problems and results in excellent agreement with the boundary-layer solution. The solution difference between the expanding boundary and fixed boundary is a result of the grid difference. For the expanding boundary, the grid is nearly aligned with contours of constant Mach number. Since the streamwise Mach number is nearly constant from plane to plane, the error is minimized and the results are an improvement over the fixed boundary.

Figure 3 shows the streamwise variation of the skin friction. Skin-friction results show that the slope of the velocity profile at the wall is different between the two formulations. The slope of the temperature profile at the wall does not differ as much, resulting in minimal differences in the heat transfer coefficient.[5] This is reasonable, since the error is in the streamwise momentum equation, which affects the streamwise velocity more than the temperature. The error in the streamwise

velocity affects the temperature through the kinetic energy, and since the calculated streamwise velocity is too large, the kinetic energy is too large, resulting in a lower than correct value of the peak temperature in the boundary layer.

The error in predicting the peak temperature may not appear catastrophic because of the good prediction of the wall heat transfer. However, parabolized methods are important for the calculation of reacting flowfields with finite reaction rates.[8] The reaction rates are usually modeled as an exponential function of temperature. Therefore, a minor discrepancy in the temperature can result in a gross error in the species concentrations.

Adiabatic Wall with Linear Viscosity Law

To evaluate the error made in skin friction, the flow over a flat plate has been computed for an adiabatic wall with a linear viscosity law instead of Sutherland's equation:

$$\frac{\mu}{\mu_0} = \frac{T}{T_0} \tag{6}$$

For this case the solution of the boundary-layer equations results in a local coefficient of skin friction that is independent of Mach number and is[9]

$$C_f = \frac{0.664}{\sqrt{Re_x}} \tag{7}$$

Solutions to the PNS equations were computed for Mach numbers 2, 4, 6, and 8, with and without the correction terms, using the finite difference code. Each case was run on a fixed grid and continued downstream until the local value of $C_f\sqrt{Re_x}$ approached its asymptotic limit, signaling the end of the weak interaction region. The difference between the corrected PNS solution and the boundary-layer solution is $<3\%$, whereas the PNS uncorrected solution resulted in a difference of up to 42% (Fig. 4). The difference between the boundary-layer solution and the uncorrected PNS solution is clearly unreasonable.

Concluding Remarks

A source of error in the implementation of Vigneron's technique with fully conservative differencing has been identified and explained by a force balance analysis. Significant errors in the skin-friction coefficient and the maximum temperature in boundary-layer profiles have been demonstrated in numerical solutions of supersonic flow over a flat plate. This type of error has a special significance in computational fluid dynamics codes that use finite rate chemical reactions since the maximum temperature controls the chemical reactions. In addition, these numerical solutions have been shown to be dependent on the grid topology. The proposed procedure eliminates these problems.

Acknowledgments

The work of the first author was supported under NASA Contract NAS1-18599. The authors thank A. Douglas Dilley for providing the boundary-layer solutions.

References

[1]Vigneron, Y. C., Rakich, J. V., and Tannehill, J. C., "Calculation of Supersonic Viscous Flow over Delta Wings with Sharp Subsonic Leading Edges," AIAA Paper 78-1137, July 1978.

[2]Newsome, R. W., Walters, R. W., and Thomas, J. L., "An Efficient Iteration Strategy for Upwind/Relaxation Solutions to the Thin-Layer Navier-Stokes Equations," AIAA Paper 87-1113, June 1987.

[3]Gielda, T. P., and McRae, D. S., "An Accurate, Stable, Explicit, Parabolized Navier-Stokes Solver for High-Speed Flows," AIAA Paper 86-1116, May 1986.

[4]Korte, J. J., "An Explicit Upwind Algorithm for Solving the Parabolized Navier-Stokes Equations," NASA TP 3050, Feb. 1991.

[5]Morrison, J. H., and Korte, J. J., "Implementation of Vigneron's Streamwise Pressure Gradient Approximation in the PNS Equations," AIAA Paper 92-0189, Jan. 1992.

[6]Lawrence, S. L., Tannehill, J. C., and Chaussee, D. S., "An Upwind Algorithm for the Parabolized Navier-Stokes Equations," AIAA Paper 86-1117, May 1986.

[7]Harris, J. E., and Blanchard, D. K., "Computer Program for Solving Laminar, Transitional, or Turbulent Compressible Boundary-Layer Equations for Two-Dimensional and Axisymmetric Flow," NASA TM 83207, Feb. 1982.

[8]Kamath, H., "Parabolized Navier-Stokes Algorithm for Chemically Reacting Flows," AIAA Paper 89-0386, Jan. 1989.

[9]Schlichting, H., *Boundary-Layer Theory*, 7th ed., McGraw-Hill, New York, 1979, p. 337.

Gaster's Transform

A. P. Roychowdhury* and B. N. Sreedhar†
Indian Institute of Technology, Kharagpur, Pin, 721302 India

I. Introduction

GASTER[1] proposed a transformation to convert the temporally growing disturbances into spatial growth rates by connecting them using group velocity, for application to hydrodynamic stability analysis. Before the development of this transform, Schubauer and Skramskad,[2] Sato,[3] and others used phase velocity as the connecting parameter between spatial and temporal amplification rates of disturbances. Freymuth[4] experimentally established the need for the use of spatial growth rates to predict the stability characteristics of free shear layer flows. Gill,[5] Michalke,[6] Gaster,[7] and Mack[8] also used the spatial growth rates in the study of stability characteristics of both incompressible and compressible flows.

Though Gaster[1] has clearly indicated that his transformation was valid for small growth rates of disturbances only, he did not explicitly indicate the range. This has led to the failure of Gaster's transformation in the prediction of the spatial growth rates when used outside the range of its applicability. Direct numerical evaluation of spatial growth rates obtained on solving the linear stability eigenvalue problem and the experimental data have shown poor comparison with spatial growth rates obtained from temporal calculations using Gaster's transformation.

This Note addresses this question of why such a discrepancy exists in the values predicted using Gaster's transformation. The transformation will be shown to be valid only very close to the neutral point corresponding to $\alpha_r = 0$ and $\alpha_i = 0$, where α is complex and represents the normal mode of decomposition of the disturbance field.

II. Derivation of Gaster's Transform

A geometric point of view will be used to highlight some of the assumptions that are not explicitly indicated by Gaster[1] in his proof that might have led to the application of the transformation outside the range of its applicability. If α = wave number, ω = wave frequency, and c = phase speed, in temporal analysis, it is assumed that $\alpha = \alpha_r$ is real, $\omega = \omega_r + i\omega_i$ and $c = c_i + ic_i$ are complex, $c_i\alpha$ is the temporal amplification rate; and in the spatial stability analysis, $c = c_r$ is real, $\omega = c\alpha = c_r\alpha_r + ic_i\alpha_i = \omega_r + i\omega_i$ is complex, and $\omega_i = \alpha_i c_r$ is the spatial amplification rate.

Received Nov. 4, 1991; revision received Dec. 9, 1992; accepted for publication Dec. 18, 1991.

*Research Scholar, Department of Aerospace Engineering. Member AIAA.

†Professor and Head, Department of Aerospace Engineering.